

Prethermalization in quenched spinor condensates

Ryan Barnett,¹ Anatoli Polkovnikov,² and Mukund Vengalattore³

¹*Joint Quantum Institute and Condensed Matter Theory Center, Department of Physics, University of Maryland, College Park, Maryland 20742, USA*

²*Department of Physics, Boston University, 590 Commonwealth Avenue, Boston, Massachusetts 02215, USA*

³*Laboratory of Atomic and Solid State Physics, Cornell University, Ithaca, New York 14853, USA*

(Received 19 September 2010; revised manuscript received 14 June 2011; published 5 August 2011)

Motivated by recent experiments, we consider the dynamics of spin-1 spinor condensates after a quantum quench from the polar to ferromagnetic state from varying the quadratic Zeeman field q . We apply the truncated Wigner approximation (TWA) to the spinor system, including all spatial and spin degrees of freedom. For short times, we find full agreement with the linearized Bogoliubov analysis. For longer times, where the Bogoliubov theory fails, we find that the system reaches a quasisteady prethermalized state. We compute the Bogoliubov spectrum about the ferromagnetic state with general q and show that the resulting finite-temperature correlation functions grossly disagree with the full TWA results, thus indicating that the system does not thermalize even over very long time scales. Finally, we show that the absence of thermalization over realistic time scales is consistent with calculations of Landau damping rates of excitations in the finite-temperature condensate.

DOI: [10.1103/PhysRevA.84.023606](https://doi.org/10.1103/PhysRevA.84.023606)

PACS number(s): 67.85.-d, 03.75.Kk, 03.75.Mn, 05.30.Rt

I. INTRODUCTION

Advances in the field of ultracold atomic gases have spurred great interest in the nonequilibrium dynamics of quantum many-body systems. The ability to engineer paradigmatic model Hamiltonians, the near perfect isolation from the environment, and the experimentally accessible time scales of evolution have made it possible to address fundamental questions about the dynamics of closed, interacting quantum many-body systems.

Of particular interest in this context is the study of a “quench” across a quantum phase transition. Here, one or more parameters of the Hamiltonian are changed rapidly, resulting in a nonequilibrium evolution of the quantum system toward the establishment of long-range order. This evolution is accompanied by a spatially inhomogeneous symmetry breaking and the formation of topological defects seeded by the quench. Accurate, time-resolved studies of such quenches are of fundamental importance to a wide range of nonequilibrium phase transitions.

Recently, an instance of such a quench across a phase transition was experimentally realized with quantum degenerate spin-1 Bose gases of ^{87}Rb [1,2]. At low magnetic fields, these multicomponent fluids are characterized by a contact interaction that favors a ferromagnetic phase. At large external magnetic fields, the quadratic Zeeman energy (QZE) dominates the interaction and favors a paramagnetic (“polar”) phase. As shown in Fig. 1, these two phases are separated by a continuous phase transition. In the experiment, *in situ* images of the spin textures following a quench of the degenerate gas into the ferromagnetic phase revealed the inhomogeneous growth of transversely magnetized domains accompanied by the sporadic observation of topological defects that were characterized as spin vortices.

Motivated by this experiment, we consider here the evolution of spin textures following a quench from the polar phase to the ferromagnetic phase. While the short-time growth of magnetization during such a quench has been analyzed [3–11], we consider here the evolution over much longer

periods and study the manner in which the spin degrees of freedom thermalize following the quench. Applying the truncated Wigner approximation (TWA) to this problem (for an overview of the TWA method and its applications, see Refs. [12,13]), we analyze the long-time dynamics of the spin degrees of freedom.

We find that unless the QZE is quenched to the immediate vicinity of the critical value corresponding to the transition to the ferromagnetic phase, the system reaches a slowly evolving quasisteady state with exponentially decaying correlations. This correlation length increases very slowly in time in a manner consistent with coarsening dynamics [14]. We also find and interpret previously unexplored physics of the dynamics of spinor condensates such as the emergence of longitudinal magnetization.

II. THE HAMILTONIAN AND MEAN-FIELD PHASES

Following the experimental situation, we consider the parameter regime characteristic of $F = 1$ spinor condensates of ^{87}Rb . Also, as in the experiment, the gases are confined in a quasi-two-dimensional (Q2D) geometry wherein the spatial extent d_y of the condensate along one dimension is less than the spin healing length. This condition implies that the spin dynamics along this axis are effectively frozen. The starting point is the Hamiltonian

$$\mathcal{H} = \mathcal{H}_0 + \mathcal{H}_{\text{int}}, \quad (1)$$

where the free Hamiltonian is

$$\mathcal{H}_0 = \int d^2r \Psi^\dagger \left(-\frac{\hbar^2}{2m} \nabla^2 + V + qf_z^2 \right) \Psi \quad (2)$$

and $\Psi = (\psi_1, \psi_0, \psi_{-1})^T$ is a three-component spinor, V is the trapping potential, $f_{x,y,z}$ are the spin-1 matrices, and q is the quadratic Zeeman shift. The interaction Hamiltonian is

$$\mathcal{H}_{\text{int}} = \int d^2r \left(\frac{1}{2} c_0 n^2 + \frac{1}{2} c_2 F^2 \right). \quad (3)$$

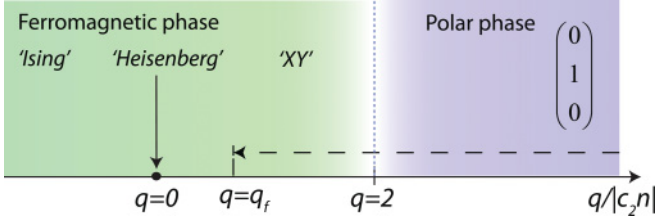


FIG. 1. (Color online) Zero-temperature phase diagram of a spin-1 Bose condensate indicating the transition from a polar phase to a ferromagnetic phase at low quadratic Zeeman energy (QZE). The dashed line indicates the direction of the quench from an initial QZE $q \gg 2|c_2|n_0$ to a final QZE $q = q_f$.

Here we have $n = \Psi^\dagger \Psi$, $\mathbf{F} = \Psi^\dagger \mathbf{f} \Psi$, and the parameters c_0 and c_2 can be expressed in terms of the s -wave scattering lengths as $c_0 = \frac{4\pi\hbar^2}{d_s 3m} (a_0 + 2a_2)$ and $c_2 = \frac{4\pi\hbar^2}{d_s 3m} (a_2 - a_0)$. There is also a linear Zeeman shift in the system proportional to F_z , but this can be dropped since F_z commutes with the Hamiltonian and thus is conserved. Spinor gases of ^{87}Rb are characterized by the scattering lengths a_0 (a_2) = 101.8 (100.4) Bohr radii, respectively. Because $a_2 < a_0$, the spin-dependent interaction in these spinor gases favors the ferromagnetic state. Since for these parameters $c_0 \gg |c_2|$, fluctuations in the total density are suppressed. Further, due to the weak spin-interaction strength, the interparticle separation at typical densities is far smaller than the spin healing length, thereby suppressing the role of quantum depletion.

III. SHORT-TIME THEORY

As illustrated in Fig. 1, for $q > q_0 \equiv 2|c_2|n_0$, the ground state is the polar state, while decreasing q below q_0 causes the ground state to acquire a magnetic moment and eventually reach the fully polarized ferromagnetic state at $q = 0$. Initially, we take $q = q_i$ to be the largest energy parameter in the Hamiltonian and quench to a final state $q = q_f$, where $0 \leq q_f < q_0$. For short times, the dynamics is expected to be well-described by expanding the Hamiltonian to quadratic order around the initial polar state [3–9], $\Psi = \sqrt{n_0}(0, 1, 0)^T$. Under this expansion, the Hamiltonian becomes

$$\mathcal{H} \approx \sum_{\mathbf{k}} [(\varepsilon_{\mathbf{k}} + c_2 n_0 + q_f)(\psi_{1,\mathbf{k}}^\dagger \psi_{1,\mathbf{k}} + \psi_{-1,\mathbf{k}}^\dagger \psi_{-1,\mathbf{k}}) + c_2 n_0 (\psi_{1,\mathbf{k}}^\dagger \psi_{-1,-\mathbf{k}}^\dagger + \psi_{-1,-\mathbf{k}} \psi_{1,\mathbf{k}})], \quad (4)$$

where we have dropped the term describing the stiff density fluctuations. For simplicity, we have considered the system in the continuum, in the absence of the trapping potential. In the ferromagnetic regime, this quadratic Hamiltonian gives modes with imaginary frequencies, which correspond to unstable, exponentially growing in time modes [3].

To quantify the spin dynamics after the quench, it is natural to consider transverse and longitudinal magnetization correlation functions,

$$G_{\perp}(\mathbf{r}, t) = \frac{1}{n_0^2} \langle : F_{+}(\mathbf{r}) F_{-}(0) : \rangle, \quad (5)$$

$$G_z(\mathbf{r}, t) = \frac{1}{n_0^2} \langle : F_z(\mathbf{r}) F_z(0) : \rangle \quad (6)$$

[3] and the concomitant gain functions, $G_{\perp}(t)$ and $G_z(t)$, which are the above evaluated for $\mathbf{r} = 0$. For $q_0 t / \hbar \gg 1$ and $q_f = 0$, the above correlations within the linearized theory give

$$G_{\perp}(t) = \frac{1}{\sqrt{8\pi} q_0 t / \hbar} \frac{1}{n_0 \xi_s^2} e^{q_0 t / \hbar}, \quad (7)$$

$$G_z(t) = \frac{1}{64\pi q_0^2 t^2 \hbar^2} \frac{1}{(n_0 \xi_s^2)^2} e^{2q_0 t / \hbar}, \quad (8)$$

where $\xi_s = \sqrt{\hbar^2 / q_0 m}$ is the spin-coherence length. Interestingly, the longitudinal gain grows with twice the exponent of the transverse gain. However, the longitudinal magnetization is suppressed by a large factor $1/(n_0 \xi_s^2) \sim 10^{-4}$ for the experimental parameters of Ref. [1]. Thus, $G_z(t)$ remains much smaller than $G_{\perp}(t)$ up to the times where the latter saturates ($G_{\perp}(t) \approx 1$ and the linearized theory does not work (see Fig. 2).

IV. TRUNCATED WIGNER SIMULATIONS

As seen from the exponential growth of the gain functions, the above theory clearly fails once the transverse magnetization is of order unity. To gain a more complete understanding, we turn to truncated Wigner simulations. This technique involves propagating the full spinor Gross-Pitaevskii equations (GPE's) of motion obtained by taking the classical limit of Eq. (1) seeded with random initial conditions for canonical degrees of freedom distributed according to the Wigner transform of the initial state. For our case, the initial state is taken to be the vacuum of Bogoliubov quasiparticles for a theory expanded about the polar state. For the limiting case of $q_i = \infty$, this has the particularly simple form $W(\Psi) \approx \delta(|\psi_{0,0}|^2 - n_0) \prod_{\mathbf{k}} 8 \exp[-2 \sum_{\alpha} |\psi_{\alpha,\mathbf{k}}|^2]$, where the factor of 8 ensures the correct normalization of the Wigner function [13].

To propagate the wave functions governed by the spinor GPE, we first discretize the system effectively by using a lattice with the constant ℓ chosen such that $\ell \ll \xi_s$ and $n_0 \ell^2 \gg 1$,

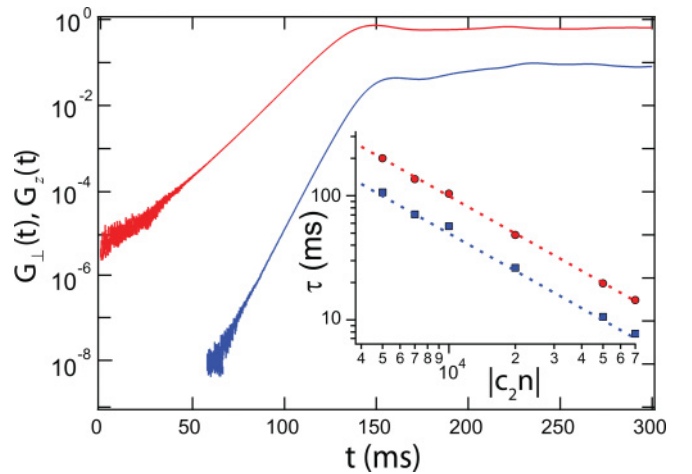


FIG. 2. (Color online) The growth of transverse (red, upper line) and longitudinal (blue, lower line) magnetization following a quench to $q_f = 0$. Inset: The characteristic time constants for the growth of transverse and longitudinal magnetization densities vs the 2D interaction strength $|c_2 n|$. The dashed lines indicate the predictions of the linearized Bogoliubov treatment for the respective parameters.

and then we use a split-operator method that is accurate up to cubic order in the time-step size [15,16]. The TWA is an approximate method resulting in the leading order in the expansion of classical dynamics in quantum fluctuations [13]. It is also known to be asymptotically accurate at short times and exact for quadratic theories. In our case, we expect this method to be quantitatively accurate at all times. Indeed, the small parameter of the expansion is $1/(n_0\xi_s^2) \ll 1$ so that quantum corrections to TWA are suppressed by this factor and are potentially only important at very long times. At longer times when nonlinearities become relevant, the momentum modes become highly occupied and the dynamics remains classical. Putting the system on a lattice ensures that there is no potential spurious effect from vacuum occupation of high-energy modes, which sometimes impedes the validity of the TWA at long times [12]. We checked that the results of our simulations are insensitive to the choice of the cutoff as long as it is shorter than the spin-coherence length.

Shown in Fig. 2 are the TWA results for the transverse and longitudinal gain functions in the absence of a trap compared with the analytic results based upon the above linearized theory. At short evolution times following the quench, the simulations predict the exponential growth of both the transverse and longitudinal magnetization densities in a manner that is in excellent agreement with the linearized theory. During this period, the spin textures are characterized by ferromagnetic domains that are predominantly oriented in the transverse plane.

V. LONG-TIME BEHAVIOR

We now move on to discuss the long-time dynamics of the quenched spinor condensate. As is seen in the gain functions in Fig. 2, the magnetization of the system eventually saturates and reaches a steady state. This motivates one to consider the prospect of thermalization in the system. More specifically, under the assumption of thermalization, the system will evolve to the ground state at $q = q_f$, with the excess energy accounted for by a superposition of elementary excitations about this configuration. We will therefore consider the theory about the state at $q = q_f$.

We define the heating (excess energy) of the system as

$$Q = \langle \mathcal{H} \rangle_i - \langle \mathcal{H} \rangle_{\text{gs}}, \quad (9)$$

where the above expectation values are evaluated for the initial state immediately after the quench and the ground state for $q = q_f$. To extract the equilibrium temperature, this heating can be compared with the thermal energy of the system. It is convenient to use the following parametrization of the spinor:

$$\Psi = \sqrt{n} e^{i\alpha} (\sin \eta \cos \phi e^{i\xi}, \cos \eta e^{i\gamma}, \sin \eta \sin \phi e^{-i\xi})^T. \quad (10)$$

With this, one can see that for $0 < q_f/q_0 < 1$, the classical energy is minimized for $\phi = \pi/4$, $\gamma = 0$, and $\cos(2\eta) = q_f/q_0$. One then obtains that the above heating is

$$Q = \frac{1}{4} N q_0 (1 - q_f/q_0)^2, \quad (11)$$

where the details of this calculation are in Appendix A. Note that the above is based on classical energy differences. In addition to this classical contribution to the heating, there

is also a quantum correction coming from the zero-point fluctuations of the condensate. However, this contribution is suppressed by a large factor $\sqrt{n_0\xi_s^2} \sim 100$ and thus is not important.

The thermal energy of the final state is found from

$$Q = U(T) \equiv \text{Tr}(e^{-\mathcal{H}/T} \mathcal{H})/Z, \quad (12)$$

where $Z = \text{Tr}(e^{-\mathcal{H}/T})$ is the partition function and the ground-state energy of the system is set to be zero. To evaluate the above, we develop a second Bogoliubov theory by expanding the Hamiltonian to quadratic order about the minimum at $q = q_f$. Note that within the chosen parametrization, one automatically avoids subtleties related to the lack of a long-range order in two dimensions at finite temperatures. The quadratic theory is then checked self-consistently by verifying that the resulting thermal depletion is small for the computed temperature.

The full Bogoliubov analysis of the spectrum linearized around the ferromagnetic minimum is rather cumbersome because of the phonon-magnon coupling [17] (which vanishes for the special points $q_f = 0$ and $q_f = q_0$). However, ^{87}Rb has a natural separation of energy scales since $c_0 \gg |c_2|$, which inhibits density fluctuations. This simplifies the Bogoliubov analysis significantly and effectively results in the decoupling of the stiff density fluctuation and the spin modes. In this limit, one finds the simplified spectrum consisting of two modes with the dispersion (see Appendix A)

$$\begin{aligned} \omega_{\mathbf{k}}^{(\perp)} &= \sqrt{\varepsilon_{\mathbf{k}}(\varepsilon_{\mathbf{k}} + q_f)}, \\ \omega_{\mathbf{k}}^{(z)} &= \sqrt{(\varepsilon_{\mathbf{k}} + q_0) \left(\varepsilon_{\mathbf{k}} + \frac{q_0^2 - q_f^2}{q_0} \right)}, \end{aligned} \quad (13)$$

where $\varepsilon_{\mathbf{k}}$ is the free-particle dispersion. Note that these reduce to the known dispersions in the limits of $q_f = 0$ and $q_f = q_0$ [18,19]. Furthermore, the large- c_0 limit of the full dispersion [17] agrees with Eq. (13). These expressions are used to compute the thermal energy of the system. It is straightforward to verify that unless q_f is very close to q_0 , $1 - q_f/q_0 \gg 1/\sqrt{n_0\xi_s^2}$, the dominant contribution to the thermal energy $U(T)$ comes from the quadratic dispersion of these modes: $\omega_{\mathbf{k}}^{(\perp)} \approx \omega_{\mathbf{k}}^{(z)} \approx \varepsilon_{\mathbf{k}}$. This can be justified *a posteriori* by comparing the temperature with q_0 . With these conditions, $U(T) \approx N\pi T^2/6(n_0\xi_s^2)q_0$. Finally, equating this to the heating, one finds

$$T = \sqrt{\frac{3}{2\pi} n_0\xi_s^2 (q_0 - q_f)}. \quad (14)$$

To test the hypothesis of thermalization, we use the developed quadratic theory to evaluate finite-temperature correlation functions [evaluated at temperature Eq. (14)] and compare with long-time TWA results. The most natural correlation function to consider is G_{\perp} defined in Eq. (5). The gapless mode, Eq. (13), which leads to algebraic decay of the correlation function in two dimensions, has the dominant contribution. Within the quadratic Bogoliubov theory, the correlation function is found to be (see Appendix B)

$$G_{\perp}(\mathbf{r}) = [1 - (q_f/q_0)^2](r/\xi_s)^{-\alpha} \quad (15)$$

with exponent $\alpha = \sqrt{6/\pi^3} \sqrt{1/n_0 \xi_s^2}$. Because of the dependence of the exponent α on the small parameter $1/n_0 \xi_s^2$, we see that, assuming equilibrium, $G_{\perp}(\mathbf{r})$ will not decay by any appreciable amount over the relevant length scales of the condensate, which are typically of the order of tens or hundreds of the spin coherence length ξ_s . For the same reason, in equilibrium the system should not have any vortices.

We point out that the resulting thermal state of the condensate with temperature T given by Eq. (14) has some interesting properties. On the one hand, except for a small vicinity of $q_f \approx q_0$, it is a high-temperature classical state characterized by a temperature much higher than the chemical potential. This implies that quantum depletion in this state is negligible. On the other hand, the smallness of the exponent α shows that this state is well below the Kosterlitz-Thouless (KT) transition temperature due to the unbinding of vortices in the spin degrees of freedom. More specifically, the KT transition temperature scales as $T_{KT} \sim q_0 n_0 \xi_s^2$, which can be compared with Eq. (14). In this respect, this is a low-temperature state.

We now compare these predictions to the results of the TWA simulations for long times. Shown in Fig. 3 are magnetizations for short and long times as well as correlation functions after the quench. Displayed are results for zero final quadratic Zeeman field $q_f = 0$, though qualitatively very similar results occur for finite values of q_f (for a full animation of the dynamics, see the supplementary material [20]). As shown

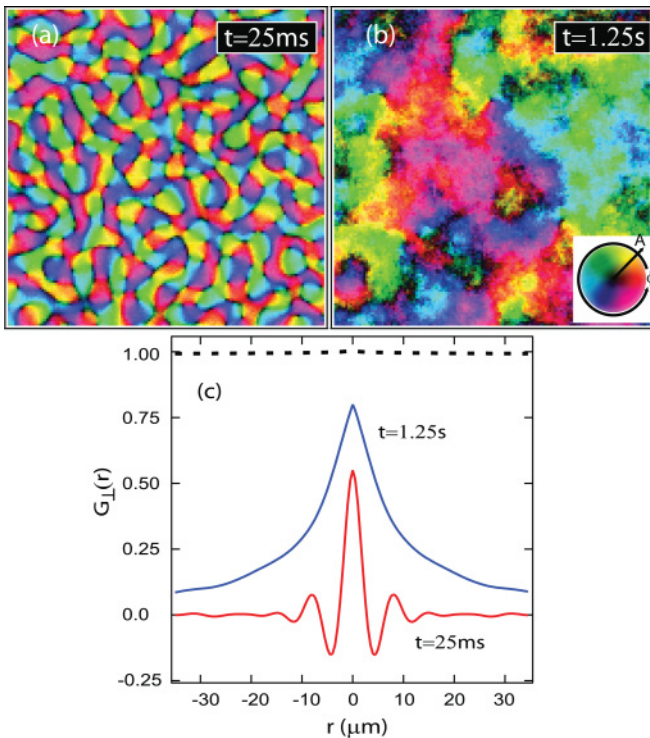


FIG. 3. (Color online) The transverse magnetization densities for short (a) and long (b) times for $q_f = 0$ over a $70 \times 70 \mu\text{m}$ region. The amplitude and orientation of the transverse magnetization are indicated by the brightness and hue (color wheel shown). (c) The spin correlation function for these same times. While the correlation function at short times is in excellent agreement with Bogoliubov theory, the decay of this function at long evolution times is much more rapid than predicted by Eq. (15) (dashed line).

in Fig. 3(c), the correlation function G_{\perp} before saturation for short times has the functional dependence of a Bessel function $J_0(r/\xi_s)$, as previously predicted [3]. For long times, the correlation function reaches a steady state and decays by over a factor of 5 from its $r = 0$ value for a system size on the order of 50 spin coherence lengths. Such decay is qualitatively incompatible with the theory developed by assuming thermalization. We thus conclude that these spinor condensate systems do not thermalize at appreciable time scales but rather reach a quasisteady (prethermalized) regime that evolves anomalously slowly in time. Such prethermalized phases were suggested earlier in the contexts of weakly interacting fermions [21,22], Bose superfluids [23,24], and the dynamics of the early Universe [25]. What is perhaps unexpected is that in this system, anomalously slow relaxation occurs at very high levels of the heating in the system.

To support these results, it is useful to compare with the Landau damping rates of long-wavelength Bogoliubov modes as a result of scattering from thermal modes [26–29]. Such an analysis is carried out in Appendix C. It is found that typical lifetimes of these modes are on the order of 100 s. This rate is considerably lower than those of scalar condensates due to the weak spin-dependent interaction and small thermal depletion. The lifetime estimates provide lower bounds for the thermalization time and are consistent with the numerical results. However, such long time scales are beyond our numerical as well as experimental access.

In conclusion, we have examined the long-time evolution of quantum degenerate spinor gases following a quench to a ferromagnetic phase. Assuming a thermalized final state, we find that the finite-temperature spin correlations are characterized by an algebraic decay over length scales much larger than the relevant length scales of the condensate. In distinct contrast, numerical simulations based on the truncated Wigner approximation indicate a rapidly decaying correlation function even at extremely long evolution times. This inconsistency leads one to the conclusion that the quenched spinor condensates will not thermalize over experimentally relevant time scales. These results are consistent with the Landau damping rates. The role of dipolar interactions [2,30] in the long-time evolution has yet to be examined.

ACKNOWLEDGMENTS

We thank E. Altman, A. Lamacraft, L. Mathey, G. Refael, J. D. Sau, and A. Turner for valuable discussions. M.V. thanks L. M. Aycok and S. Chakram for valuable discussions and critical comments on the manuscript. We gratefully acknowledge financial support from the NSF JQI Physics Frontier Center and the Sherman Fairchild Foundation (R.B.), AFOSR FA9550-10-1-0110 and the Sloan Foundation (A.P.), and Cornell University (M.V.). The authors also gratefully acknowledge the hospitality of the Aspen Center for Physics, where a part of this work was completed.

APPENDIX A: BOGOLIUBOV ANALYSIS IN THE REGIME

$$0 < q_f < 2|c_2|n_0$$

The easiest way to perform the Bogoliubov analysis of spinor condensates is to use a parametrization of the spinors

though the density-angle variables as in Eq. (10). In this case, one avoids issues related to absence of the true condensation in one dimension at finite temperatures. Also, the normal modes have a very transparent physical meaning. The analysis of this appendix mimics very closely an analysis for the description of the low-energy excitations of bosons in an optical lattice close to the superfluid-insulator transition in the effective spin-1 representation [31,32]. In this parametrization, the magnetizations $F_z = \Psi^* f_z \Psi$ and $F_{z,2} = \Psi^* f_z^2 \Psi$ are given by

$$F_z = |\Psi_1|^2 - |\Psi_{-1}|^2 = n \sin^2(\eta) \cos(2\phi), \quad (\text{A1})$$

$$F_{z,2} = |\Psi_1|^2 + |\Psi_{-1}|^2 = n \sin^2(\eta). \quad (\text{A2})$$

Similarly, the square of the transverse magnetization $|F_\perp|^2 = F_y^2 + F_x^2$ reads

$$|F_\perp|^2 = \frac{n^2}{2} \sin^2(2\eta)[1 + \sin(2\phi) \cos(2\gamma)]. \quad (\text{A3})$$

With these expressions, one finds for the interaction energy density (here we include the quadratic Zeeman term in the interaction energy)

$$\begin{aligned} \mathcal{H}_{\text{int}} &= \frac{c_0}{2} n^2 + \frac{c_2}{2} (F_z^2 + |F_\perp|^2) + q F_{z,2} \\ &= \frac{c_0}{2} n^2 + c_2 n^2 \sin^2(\eta) \cos^2(\eta) [1 + \sin(2\phi) \cos(2\gamma)] \\ &\quad + q n \sin^2(\eta) + \frac{c_2 n^2}{2} \sin^4(\eta) \cos^2(2\phi). \end{aligned} \quad (\text{A4})$$

It is straightforward to check that for $c_2 < 0$ and $0 < q < 2|c_2|n = q_0$, the energy is minimized when $\phi = \pi/4$, $\gamma = 0$, and $\eta = \bar{\eta}$, where we define $\bar{\eta}$ according to $q = q_0 \cos(2\bar{\eta})$. There is an equivalent minimum obtained by gauge transformation where $\phi \rightarrow \phi + \pi/2$ and $\gamma \rightarrow \gamma + \pi$. The minimum of the interaction energy density is then

$$E(q) \approx -q_0 n \sin^4(\bar{\eta}) = -\frac{g_0 n}{4} \left(1 - \frac{q}{q_0}\right)^2. \quad (\text{A5})$$

Note that in this expression we ignored the zero-point energy associated with the depletion, which is suppressed by a large factor $1/\sqrt{n_0 \xi_s^2}$.

Within the Bogoliubov approximation, we need to expand the energy around the minimum. For this purpose, we define small deviations of the angles ϕ and η from the optimal values $\phi = \pi/4 + \delta\phi$, $\eta = \bar{\eta} + \delta\eta$ and do a second-order expansion in $\delta\phi$, $\delta\eta$, γ , and ξ . Since we are interested in the limit $c_0 \gg c_2$, the density fluctuations are suppressed and we can set $\delta n = 0$ and fix the density at its equilibrium value $n = n_0$. Then the expression for the interaction energy density (A4) reduces to

$$\begin{aligned} \delta \mathcal{H}_{\text{int}} &\approx q_0 n_0 \sin^2(\bar{\eta}) [\cos(2\bar{\eta})(\delta\phi)^2 \\ &\quad + \cos^2(\bar{\eta})\gamma^2 + 4 \cos^2(\bar{\eta})(\delta\eta)^2]. \end{aligned} \quad (\text{A6})$$

Under the same approximation, the kinetic-energy density term reads

$$\begin{aligned} \mathcal{H}_{\text{kin}} &\approx \frac{\hbar^2}{2m} [(\nabla\delta\eta)^2 + \sin^2(\bar{\eta})(\nabla\phi)^2 + \sin^2(\bar{\eta})(\nabla\xi)^2 \\ &\quad + \cos^2(\bar{\eta})(\nabla\gamma)^2 + (\nabla\alpha)^2 + 2\nabla\alpha\nabla\gamma \cos^2(\bar{\eta})]. \end{aligned} \quad (\text{A7})$$

And finally, to determine the canonically conjugate variables, we need to write the Berry phase term $i\Psi^\dagger \dot{\Psi}$ in the linearized approximation,

$$2n_0 \sin^2(\bar{\eta}) \delta\phi \dot{\xi} + n_0 \sin(2\bar{\eta}) \delta\eta \dot{\gamma} - \delta n [\dot{\alpha} + \cos^2(\bar{\eta}) \dot{\gamma}]. \quad (\text{A8})$$

In this form, it is clear that the phase conjugate to the density fluctuations is $\tilde{\alpha} = \alpha + \cos^2(\bar{\eta})\gamma$. Then the kinetic energy density can be rewritten as

$$\begin{aligned} \mathcal{H}_{\text{kin}} &\approx \frac{\hbar^2}{2m} n_0 [(\nabla\eta)^2 + \sin^2(\bar{\eta})(\nabla\phi)^2 + \sin^2(\bar{\eta})(\nabla\xi)^2 \\ &\quad + (\nabla\tilde{\alpha})^2 + \cos^2(\bar{\eta}) \sin^2(\bar{\eta})(\nabla\gamma)^2]. \end{aligned} \quad (\text{A9})$$

One can further redefine the variables

$$\begin{aligned} \delta\phi &\rightarrow \tilde{\phi}/[2\sqrt{n_0} \sin(\bar{\eta})], \quad \xi \rightarrow \tilde{\xi}/\sqrt{n_0} \sin(\bar{\eta}), \\ \gamma &\rightarrow \tilde{\gamma}/\sqrt{n_0} \sin(2\bar{\eta}), \quad \eta \rightarrow \tilde{\eta}/\sqrt{n_0}. \end{aligned}$$

Then, the spin part of the Lagrangian density (Berry phase minus Hamiltonian) becomes

$$\begin{aligned} \mathcal{L} &\approx \tilde{\phi} \dot{\tilde{\xi}} + \tilde{\eta} \dot{\tilde{\gamma}} - g_s \left[\frac{\cos(\bar{\eta}/2)}{4} \tilde{\phi}^2 + \cos^2(\bar{\eta}) \tilde{\gamma}^2 + \sin^2(2\bar{\eta}) \tilde{\eta}^2 \right] \\ &\quad - \frac{\hbar^2}{2m} \left[(\nabla\tilde{\eta})^2 + \frac{1}{4} (\nabla\tilde{\phi})^2 + (\nabla\tilde{\xi})^2 + \cos^2(\bar{\eta})(\nabla\tilde{\gamma})^2 \right]. \end{aligned} \quad (\text{A10})$$

This Lagrangian density immediately gives two sets of normal modes corresponding to oscillations in the ϕ - ξ variables, which represent uniform rotations around the z axis, and in the η - γ variables, which represent oscillations in the magnitude of the transverse magnetization. The corresponding frequencies in momentum space are

$$\omega_{\mathbf{k}}^{(\perp)} = \sqrt{\varepsilon_{\mathbf{k}} [\varepsilon_{\mathbf{k}} + q_0 \cos(2\bar{\eta})]}, \quad (\text{A11})$$

$$\omega_{\mathbf{k}}^{(z)} = \sqrt{(g_0 + \varepsilon_{\mathbf{k}}) [\varepsilon_{\mathbf{k}} + q_0 \sin^2(2\bar{\eta})]}, \quad (\text{A12})$$

where $\varepsilon_{\mathbf{k}} = \frac{\hbar^2 k^2}{2m}$ is the free-particle dispersion. We note that these expressions follow from taking the $c_0 \rightarrow \infty$ limit of the general dispersion relations obtained in Ref. [17]. There are, however, advantages to using the density-angle representation since it does not rely on the assumption of the existence of true long-range order.

APPENDIX B: FINITE-TEMPERATURE CORRELATION FUNCTIONS WITHIN THE BOGOLIUBOV THEORY

The Bogoliubov theory described in the previous section makes it possible to compute correlation functions in two-dimensional systems. In the following, we will consider the transverse magnetization correlation function

$$G_\perp(\mathbf{r}, t) = \frac{1}{n_0^2} \langle : F_+(\mathbf{r}) F_-(0) : \rangle. \quad (\text{B1})$$

Written in terms of the variables introduced in the previous section, we have

$$F_+ = \frac{1}{\sqrt{2}} n e^{i\alpha} \sin(2\eta) e^{-i\xi} [\cos(\phi) e^{i\gamma} + \sin(\phi) e^{-i\gamma}]. \quad (\text{B2})$$

According to the Mermin-Wagner theorem, a gapless mode will lead to a power-law behavior of correlation functions in two dimensions. The gapless mode for our case corresponds to the ϕ - ξ variables. It is straightforward to see that these will dominate the correlation functions. Taking into account these two fluctuating fields, one finds

$$\langle F_+(\mathbf{r})F_-(0) \rangle = \sin^2(2\bar{\eta})e^{-\langle \Delta\phi^2 \rangle/2}e^{-\langle \Delta\xi^2 \rangle/2}. \quad (\text{B3})$$

In this equation, $\langle \Delta\xi^2 \rangle \equiv \langle [\xi(\mathbf{r}) - \xi(0)]^2 \rangle$ with a similar expression for $\langle \Delta\phi^2 \rangle$.

Using the above analysis, one finds

$$\langle \Delta\xi^2 \rangle = \frac{1}{N \sin^2(\bar{\eta})} \sum_{\mathbf{k}} \frac{\omega_{\mathbf{k}}^{(\perp)}}{\varepsilon_{\mathbf{k}}} [f(\omega_{\mathbf{k}}^{(\perp)}) + 1/2][1 - J_0(kr)] \quad (\text{B4})$$

and

$$\langle \Delta\phi^2 \rangle = \frac{1}{N \sin^2(\bar{\eta})} \sum_{\mathbf{k}} \frac{\varepsilon_{\mathbf{k}}}{\omega_{\mathbf{k}}^{(\perp)}} [f(\omega_{\mathbf{k}}^{(\perp)}) + 1/2][1 - J_0(kr)], \quad (\text{B5})$$

where f is the Bose distribution function. It can be seen that the dominant contribution comes from $\langle \Delta\xi^2 \rangle$ due to the long-wavelength divergence of the sum over \mathbf{k} , which is cut off at $\sim 1/r$. The above expression is therefore well-approximated by

$$\langle \Delta\xi^2 \rangle = \frac{T}{\pi \sin^2(\bar{\eta})q_0 n_0 \xi_s^2} \ln(r/\xi_s). \quad (\text{B6})$$

Using the expression for the temperature derived in the paper, one arrives at Eq. (15).

APPENDIX C: LANDAU DAMPING RATE

We take a spinor condensate with a single Bogoliubov excitation of wave vector \mathbf{k} and evaluate its lifetime τ_k due to scattering off of short-wavelength thermal modes. For simplicity, we will consider the gapless spin mode $\omega_{\mathbf{k}}^{\perp}$ as given in Eq. (13). Such a rate is given by the well-known Landau damping formula [26], which has been generalized to Bose-Einstein condensates in [27–29]

$$\frac{1}{\tau_k} = \frac{\pi}{\hbar} \sum_{\mathbf{k}'} |M_{\mathbf{k}\mathbf{k}'}|^2 [f(\omega_{\mathbf{k}}^{(\perp)}) - f(\omega_{\mathbf{k}+\mathbf{k}'}^{(\perp)})] \times \delta(\omega_{\mathbf{k}}^{(\perp)} + \omega_{\mathbf{k}'}^{(\perp)} - \omega_{\mathbf{k}+\mathbf{k}'}^{(\perp)}), \quad (\text{C1})$$

where f is the Bose-Einstein distribution function. In this equation, the matrix element $M_{\mathbf{k}\mathbf{k}'}$ is given by [27–29]

$$M_{\mathbf{k}\mathbf{k}'} = \frac{q_f}{2\sqrt{N}} \sqrt{\frac{\hbar k}{2ms}} \left(\frac{\varepsilon_{\mathbf{k}'}}{\omega_{\mathbf{k}'}^{(\perp)}} + \frac{\omega_{\mathbf{k}'}^{(\perp)}}{\varepsilon_{\mathbf{k}'} + q_f/2} \right), \quad (\text{C2})$$

where s is the sound speed of the mode $\omega_{\mathbf{k}'}^{(\perp)}$. With this expression, the two-dimensional \mathbf{k}' summation can be performed. In the limit $T \gg q_f$, the result is

$$\frac{1}{\tau_k} = \frac{a_s k}{\hbar} \frac{T}{d_y/\xi_s} \frac{q_f}{q_0} 1.13 = \frac{k\xi_s}{\hbar} \frac{T}{8\pi n_0 \xi_s^2} \frac{q_f}{q_0} 1.13, \quad (\text{C3})$$

where $a_s = (a_2 - a_0)/3$ is the spin-dependent scattering length. Using the experimental parameters and the expression for the temperature given in Eq. (14), and taking $q_f = q_0/2$, we find that

$$\tau_k \approx 90 \text{ s} \quad (\text{C4})$$

for a mode having a wave vector $q = 1/(2\xi_s)$.

-
- [1] L. E. Sadler, J. M. Higbie, S. R. Leslie, M. Vengalattore, and D. M. Stamper-Kurn, *Nature (London)* **443**, 312 (2006).
- [2] M. Vengalattore, S. R. Leslie, J. Guzman, and D. M. Stamper-Kurn, *Phys. Rev. Lett.* **100**, 170403 (2008).
- [3] A. Lamacraft, *Phys. Rev. Lett.* **98**, 160404 (2007).
- [4] H. Saito, Y. Kawaguchi, and M. Ueda, *Phys. Rev. A* **76**, 043613 (2007).
- [5] B. Damski and W. H. Zurek, *Phys. Rev. Lett.* **99**, 130402 (2007).
- [6] M. Uhlmann, R. Schützhold, and U. R. Fischer, *Phys. Rev. Lett.* **99**, 120407 (2007).
- [7] R. W. Cherng, V. Gritsev, D. M. Stamper-Kurn, and E. Demler, *Phys. Rev. Lett.* **100**, 180404 (2008).
- [8] M. Baraban, H. F. Song, S. M. Girvin, and L. I. Glazman, *Phys. Rev. A* **78**, 033609 (2008).
- [9] C. Klempt, O. Topic, G. Gebreyesus, M. Scherer, T. Henninger, P. Hyllus, W. Ertmer, L. Santos, and J. J. Arlt, *Phys. Rev. Lett.* **103**, 195302 (2009).
- [10] H. Saito, Y. Kawaguchi, and M. Ueda, *Phys. Rev. A* **75**, 013621 (2007).
- [11] J. D. Sau, S. R. Leslie, D. M. Stamper-Kurn, and M. L. Cohen, *Phys. Rev. A* **80**, 023622 (2009).
- [12] P. B. Blakie, A. S. Bradley, M. J. Davis, R. J. Ballagh, and C. W. Gardiner, *Adv. Phys.* **57**, 353 (2008).
- [13] A. Polkovnikov, *Ann. Phys. (NY)* **325**, 1790 (2010).
- [14] A. J. Bray, *Adv. Phys.* **43**, 357 (1994).
- [15] J. Javanainen and J. Ruostekoski, *J. Phys. A* **39**, L179 (2006).
- [16] R. Barnett, E. Chen, and G. Refael, *New J. Phys.* **12**, 043004 (2010).
- [17] S. Uchino, M. Kobayashi, and M. Ueda, *Phys. Rev. A* **81**, 063632 (2010).
- [18] T.-L. Ho, *Phys. Rev. Lett.* **81**, 742 (1998).
- [19] T. Ohmi and K. Machida, *J. Phys. Soc. Jpn.* **67**, 1822 (1998).
- [20] R. Barnett, A. Polkovnikov, and M. Vengalattore (unpublished); See Supplemental Material at <http://link.aps.org/supplemental/10.1103/PhysRevA.84.023606> for the full animation of the dynamics.
- [21] M. Moeckel and S. Kehrein, *New J. Phys.* **12**, 055016 (2010).
- [22] M. Eckstein, M. Kollar, and P. Werner, *Phys. Rev. Lett.* **103**, 056403 (2009).
- [23] L. Mathey and A. Polkovnikov, *Phys. Rev. A* **81**, 033605 (2010).
- [24] T. Kitagawa, A. Imambekov, J. Schmiedmayer, and E. Demler, e-print arXiv:1104.5631.

- [25] J. Berges, S. Borsányi, and C. Wetterich, *Phys. Rev. Lett.* **93**, 142002 (2004).
- [26] E. M. Lifshitz and L. Pitaevskii, *Physical Kinetics* (Pergamon, Oxford, 1981).
- [27] L. Pitaevskii and S. Stringari, *Phys. Lett. A* **235**, 298 (1997).
- [28] S. Giorgini, *Phys. Rev. A* **57**, 2949 (1998).
- [29] C. J. Pethick and H. Smith, *Bose-Einstein Condensation in Dilute Gases* (Cambridge University Press, Cambridge, 2008).
- [30] M. Vengalattore, J. Guzman, S. R. Leslie, F. Serwane, and D. M. Stamper-Kurn, *Phys. Rev. A* **81**, 053612 (2010).
- [31] E. Altman, Ph.D. thesis, Technion University, 2002.
- [32] E. Altman and A. Auerbach, *Phys. Rev. Lett.* **89**, 250404 (2002).